Biophysical Chemistry, 45 (1992) 119–132
Elsevier Science Publishers B.V., Amsterdam

BIOCHE 01703

Refinement of the omega analysis for the characterization of solute self-association by sedimentation equilibrium

Michael P. Jacobsen and Donald J. Winzor

Department of Biochemistry, University of Queensland, Brisbane, Qld. 4072 (Australia)

(Received 19 February 1992; accepted in revised form 29 June 1992)

Abstract

A modified method of analysis is presented which improves the potential of the omega function [B.K. Milthorpe, P.D. Jeffrey and L.W. Nichol, Biophys. Chem. 3 (1975) 169] for the characterization of solute self-association by sedimentation equilibrium. Its application to reversible dimerization is illustrated by analysis of Rayleigh interferograms for α-chymotrypsin in acetate–chloride buffer (pH 3.9, I 0.2), a system for which allowance for effects of thermodynamic non-ideality is made on the statistical-mechanical basis of excluded volume. Potential use of the revised procedure for the characterization of discrete self-association involving species larger than dimer is then explored by its application to simulated data for monomer–tetramer and monomer–dimer–trimer systems. An analysis of Rayleigh interferograms for diisopropyl-α-chymotrypsin at low ionic strength (pH 7.9, I 0.03) is also presented to illustrate the characterization of a system in which the solute is considered to undergo indefinite self-association. Finally, the equivalence of quantitative inferences based on the omega analysis and the simulation of concentration distributions at sedimentation equilibrium [M.L. Johnson, J.J. Correia, D.A. Yphantis and H.R. Halvorson, Biophys. J. 36 (1981) 575] is illustrated by an adaptation of the latter procedure to obtain the association constant for α-chymotrypsin dimerization in acetate–chloride buffer, pH 3.9, I 0.2.

Keywords: Sedimentation equilibrium; Solute self-association; Omega analysis

1. Introduction

The characterization of solute self-association equilibria by sedimentation equilibrium is usually based on assessment of the concentration dependence of the weight-average molecular weight [1–11] by a procedure devised initially [12] for the analysis of light-scattering data. An obvious disadvantage of this method for the analysis of sedimentation equilibrium distributions is that the molecular weight data are obtained by differentiating a logarithmic transform of the concentration distribution with respect to the square of radial distance. Realization that such differentiation magnifies any experimental uncertainty inherent in the measured concentration distribution has led to the development of elaborately programmed software for smoothing data [13]. Although resort to such practice is undoubtedly

Correspondence to: Dr. D.J. Winzor, Department of Biochemistry, University of Queensland, Brisbane, Qld. 4072, Australia. Fax 61-7-365 1499.

necessary from the viewpoint of minimizing error in the differentiation process and hence in the experimentally assessed concentration dependence of molecular weight, the need for so doing is rendered redundant by the fact that the next step of the procedure entails reintegration of the molecular weight data to determine the weight-fraction of monomer in a solution with total solute concentration $\bar{c}(r)$.

Direct analysis of the equilibrium concentration distribution [14,15] is clearly the method of choice for obviating the additional error introduced by the above cycle of differentiation and integration to determine monomer concentration. However, the significance of the omega analysis [14] is still being either overlooked or ignored. For example, in a recent review of sedimentation equilibrium [16] a footnote was used to dismiss the omega analysis as an oddity of the Australasian scene. On the contrary, it could be argued that the omega function has been the most important breakthrough since the pioneering investigations of Adams and Williams [1] into the quantitative characterization of solute self-association by analysis of sedimentation equilibrium distributions; and that its only serious rival for that honour is the elaborate non-linear curve-fitting program devised by the Yphantis group [15] for evaluating self-association constants by simulation of the $\bar{c}(r)$–r distribution.

The virtue of the omega function, which is evaluated directly from the concentration distribution at sedimentation equilibrium, is that it provides a simple means of estimating unequivocally the thermodynamic activity of monomer as a function of total solute concentration throughout the equilibrium distribution — information that no other procedure has the capacity to provide. Admittedly, a drawback of the original version of the omega analysis [14] is the extent of reliance placed upon the accuracy of an extrapolation of the omega function to zero solute concentration, this being a problem addressed by Morris and Ralston [17,18] in their attempt to alleviate that limitation. In similar vein, we develop further the analysis from its original form [14] so that results may be assessed more accurately and conveniently.

2. The omega analysis

The omega function, $\Omega(r)$, is an experimental parameter defined by the relationship [14]

$$\Omega(r) = \left[\bar{c}(r)/\bar{c}(r_F)\right] \exp\left\{\phi M_1\left(r_F^2 - r^2\right)\right\} \quad (1a)$$

$$\phi = (1 - \bar{v}\rho_s)\omega^2/(2RT) \quad (1b)$$

in which $\bar{c}(r)$ and $\bar{c}(r_F)$ denote the respective total solute concentrations (g/L) at radial distance r and reference radial position r_F. The exponent in eq. (1a) is calculated on the basis of a molecular weight M_1 for self-associating monomer and a partial specific volume $\bar{v}$ of the solute, which is considered to be the same for monomer and all polymeric states — an assumption inherent in most analyses of sedimentation equilibrium distributions for self-associating systems [1–11,13–18]. R is the universal gas constant and T the absolute temperature in a sedimentation equilibrium experiment conducted at angular velocity ω: ρ_s is the solvent density [19–21]. In the context of quantifying solute self-association, the important feature of the omega function is its relationship to solution composition. Specifically,

$$\Omega(r) = z_1(r_F)\bar{c}(r)/\left[z_1(r)\bar{c}(r_F)\right] \quad (2a)$$

$$= \Omega_0\bar{c}(r)/z_1(r) \quad (2b)$$

where $z_1(r)$ and $z_1(r_F)$ refer to the thermodynamic activities of monomer at the respective radial positions: eq. (2b) follows from the demonstration [14] that the ratio $z_1(r_F)/\bar{c}(r_F)$ is given by the ordinate intercept, Ω_0, of a plot of $\Omega(r)$ versus $\bar{c}(r)$. The thermodynamic activity of monomer, $z_1(r)$, throughout the concentration distribution may then be calculated by noting that the condition of sedimentation equilibrium requires conformity with the expression

$$z_1(r) = z_1(r_F) \exp\left\{\phi M_1\left(r^2 - r_F^2\right)\right\} \quad (3)$$

Combination of eqs. (2) and (3) leads to the relationship

$$z_1(r) = \Omega_0\bar{c}(r_F) \exp\left\{\phi M_1\left(r^2 - r_F^2\right)\right\}. \quad (4)$$

Furthermore, $\bar{c}(r)$ may be expanded in terms of

individual species activities, $z_i(r)$, as

$$\bar{c}(r) = z_1(r)/\gamma_1(r) + \sum_2^n \left[X_i \{z_1(r)\}^i / \gamma_i(r) \right] \quad (5)$$

where the activity of each polymeric species is expressed as the product of the association constant X_i ($L^{i-1}g^{1-i}$) and the monomeric activity raised to the appropriate power: $\gamma_1(r)$ and $\gamma_i(r)$ are the respective activity coefficients of monomer and pertinent oligomeric species. With these substitutions eq. (2b) becomes

$$\Omega(r)\gamma_1(r) = \Omega_0 + \sum_2^n X_i \Omega_0^i \left[\bar{c}(r_F) \exp\{\phi M_1(r^2 - r_F^2)\} \right]^{i-1} \times \left[\gamma_1(r)/\gamma_i(r) \right] \quad (6)$$

This expression is to provide the bases for the revised procedures for quantifying a range of situations encountered in sedimentation equilibrium studies.

3. Applications of the omega analysis

In its original form [14] the omega analysis entailed extrapolation of the $\Omega(r) - \bar{c}(r)$ dependence to zero solute concentration to obtain Ω_0; and hence (via eq. 2) the activity of monomer, $z_1(r_F)$ in the solution with total solute concentration $\bar{c}(r_F)$ at the reference radial position. Since eq. (3) was then used to calculate monomeric activities, $z_1(r)$, at radial positions throughout the equilibrium distribution, heavy reliance was indeed placed on the accuracy of that nonlinear extrapolation to obtain Ω_0 [17,18]. We have therefore sought means to improve this aspect of the omega analysis – a task which necessitates the consideration of a series of separate situations.

3.1 Non-ideality of a non-associating solute

The simplest case worthy of consideration is the characterization of the thermodynamic non-ideality of a non-associating solute with molecular weight M_1. This situation is described quantitatively by setting $X_i = 0$ in eq. (6), which then becomes

$$\Omega(r) = \Omega_0/\gamma_1(r) \quad (7)$$

For moderate concentrations the virial expansion of the activity coefficient as a power series in concentration may be truncated after the linear term, whereupon eq. (7) may be rewritten as

$$\Omega(r) = \Omega_0 \exp\{-[\alpha_{11}c_1(r) + \cdots]\} \approx \Omega_0\{1 - \alpha_{11}c_1(r) + \cdots\} \quad (8)$$

in which α_{11} is the second virial coefficient (expressed in L/g) for solute self-interaction, and in which the overbar notation for total concentration has been omitted because there is only one solute. From the predicted linear dependence of $\Omega(r)$ upon solute concentration, α_{11} may be calculated as the ratio of the slope ($-\Omega_0\alpha_{11}$) to the ordinate intercept (Ω_0).

Use of the $\Omega(r)$ function for quantifying the thermodynamic non-ideality of a non-associating solute has already been illustrated in a sedimentation equilibrium study of isoelectric ovalbumin [22]. Indeed, inspection of Fig. 2a therein shows that the linear plot of $\Omega(r)$ *versus* $c_1(r)$ was used to evaluate Ω_0 and hence the thermodynamic activity, $z_1(r_F)$, of ovalbumin at the reference radial position with a concentration, $c_1(r_F)$, of 1.25 mg/ml. However, whereas the resulting value of $z_1(r_F)$, *i.e.*, $\Omega_0 c_1(r_F)$, was then used to generate the dependence of $z_1(r)$ upon $c_1(r)$ via eq. (4) so that the dependence of ln $\gamma_1(r)$ upon $c_1(r)$ could be determined (Fig. 2b of [22]), inspection of eq. (8) indicates the redundancy of such action. Clearly, α_{11} may be calculated directly from the linear dependence of $\Omega(r)$ upon $c_1(r)$. From Fig. 1, which is derived from Fig. 2a of [22], the ratio of the slope to the ordinate intercept yields a value of 0.0112 ($\pm$0.0004) L/g for α_{11}, or a second virial coefficient of 500 ($\pm$20) L/mol for the self-interaction of ovalbumin.

3.2 Characterization of solute dimerization

We first consider the situation in which the reversible dimerization of a solute is investigated

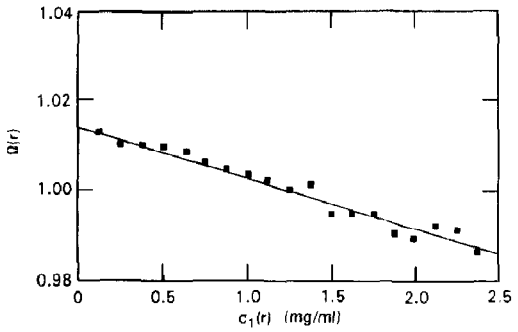

Fig. 1. Evaluation of the activity coefficient of isoelectric ovalbumin by analysis of a sedimentation equilibrium distribution in terms of the omega function (eq. 1a with $c_1(r_F) = 1.25$ mg/ml, $r_F = 7.100$ cm) and eq. (7), the data being inferred from Fig. 2a of [22].

at sufficiently low concentrations for the effect of thermodynamic nonideality to be neglected. Under those circumstances ($n = 2$, $\gamma_1(r) = \gamma_2(r) \approx 1$), eq. (6) becomes

$$\Omega(r) = \Omega_0 + X_2\Omega_0^2\bar{c}(r_F)\exp\left[\phi M_1\left(r^2 - r_F^2\right)\right] \tag{9}$$

which indicates that $\Omega(r)$ should exhibit linear dependence upon $\bar{c}(r_F)\exp[\phi M_1(r^2 - r_F^2)]$. The dimerization constant, X_2 (L/g), may thus be evaluated from the the ratio of the slope ($X_2\Omega_0^2$) to the square of the ordinate intercept (Ω_0).

Although assumed thermodynamic non-ideality is an allowable approximation in sedimentation equilibrium experiments conducted with relatively low solute concentrations, the extension of measurements to encompass a larger range of $\bar{c}(r)$ clearly brings into question the validity of that assumption; and hence draws attention to the need for an analysis that takes into account the effects of thermodynamic non-ideality.

From the relevant form of eq. (6) for a dimerizing system, namely,

$$\Omega(r)\gamma_1(r) = \Omega_0 + X_2\Omega_0^2\left\{\bar{c}(r)\exp\left[\phi M_1\left(r^2 - r_F^2\right)\right]\right\} \times\{\gamma_1(r)/\gamma_2(r)\} \tag{10}$$

it is evident that estimates of $\gamma_1(r)$ and $\gamma_2(r)$ are required for an unequivocal value of X_2 to be obtained. In that regard the traditional approach to this problem has been to adopt the simplifying assumption that the composition dependence of activity coefficients is described by the expression [23]

$$\gamma_i(r) = \exp\left[iBM_1\bar{c}(r)\right] \tag{11}$$

in which B is an empirical curve-fitting parameter. However, this description of the composition dependence of activity coefficients was introduced to allow identification of the apparent association constant based on species concentrations with the true thermodynamic constant based on species activities. Since these two parameters are inter-related by the expression

$$X_2 = X_2^{app}\left\{\gamma_2(r)/\left[\gamma_1(r)\right]^2\right\} \tag{12}$$

the adoption of eq. (11) for $\gamma_1(r)$ and $\gamma_2(r)$ leads to a value of unity for the activity coefficient ratio term. As noted previously [24], eq. (11) is an inappropriate description of the composition dependence of activity coefficients for globular proteins because B (the supposed second virial coefficient) cannot be regarded as a constant.

We therefore prefer to adopt the viewpoint that $\gamma_1(r)$ and $\gamma_2(r)$ may be obtained on the statistical-mechanical basis of excluded volume. On the basis of spherical geometry for all species, the expressions for the activity coefficients are [21]

$$\gamma_1(r) = \exp\left\{(\alpha_{11}/M_1)c_1(r) + (\alpha_{12}/M_2)\left[\bar{c}(r) - c_1(r)\right]\right\} \tag{13a}$$

$$\gamma_2(r) = \exp\left\{(\alpha_{22}/M_2)\left[\bar{c}(r) - c_1(r)\right] + (\alpha_{12}/M_1)c_1(r)\right\} \tag{13b}$$

$$\alpha_{11} = 32\pi NR_1^3/3 + Z_1^2(1 + 2\kappa R_1)/\left[2I(1 + \kappa R_1)^2\right] \tag{13c}$$

$$\alpha_{22} = 32\pi NR_2^3/3 + Z_2^2(1 + 2\kappa R_2)/\left[2I(1 + \kappa R_2)^2\right] \tag{13d}$$

$$\alpha_{12} = 4\pi N(R_1 + R_2)^3/3 + \frac{Z_1Z_2(1 + \kappa R_1 + \kappa R_2)}{2I(1 + \kappa R_1)(1 + \kappa R_2)} \tag{13e}$$

where $c_1(r)$ is the weight-concentration of monomer associated with total concentration $\bar{c}(r)$, and the charge–charge term is defined in standard Debye–Hückel nomenclature: Z_1, Z_2 and R_1, R_2 are the respective nett charges (valences) and radii of monomer and dimer with molecular weights M_1 and M_2; and the inverse screening length (κ) is related to ionic strength I by the relationship $\pi = 3.27 \times 10^7 \sqrt{I}$ at 20°C. Since the evaluation of activity coefficients, $\gamma_i(r)$, clearly requires knowledge of $c_1(r)$, the concentration of monomer at radial distance r, a logical approach is to assume thermodynamic ideality $[\gamma_1(r) = \gamma_2(r) = 1]$ initially so that first estimates of X_2 and hence $c_1(r)$ may be obtained for substitution into eq. (13) to obtain $\gamma_1(r)$ for each $\bar{c}(r)$. After plotting the results in accordance with eq. (9), we may then employ eq. (10) to obtain second estimates of Ω_0 and X_2. Should the magnitudes of Ω_0 and X_2 differ significantly from the initial estimates, their values may be refined further by successive iteration on the basis of the revised values of Ω_0 and X_2.

The feasibility of using this procedure is illustrated by reanalysis of Rayleigh interferograms obtained in an earlier sedimentation equilibrium study of α-chymotrypsin [25] under conditions (pH 3.9, I 0.2) where this enzyme undergoes reversible dimerization [25–28]. Open symbols in Fig. 2 summarize the analysis of high-speed (squares) and low-speed (circles) sedimentation equilibrium distributions in accordance with ideal sedimentation equilibrium behaviour (eq. 9) on the basis that $\bar{c}(r_F) = 1.10$ mg/mL, $M_1 = 25\,000$ and $\bar{v} = 0.736$ mL/g. Initial estimates of 0.441 and 2.56 L/g are obtained for Ω_0 and X_2 respectively. This estimate of the dimerization constant is slightly smaller than, but in reasonable agreement with, that of 3.5 L/g reported [25] on the basis of an Ω_0 value obtained by extrapolation of the curvilinear plot of $\Omega(r)$ *versus* $\bar{c}(r)$ to zero concentration.

Because the upper limit of $\bar{c}(r)$ in these experiments was 6.5 mg/mL, the consequences of thermodynamic non-ideality were assessed by resort to eq. (13) so that the data could be replotted in accordance with eq. (10) to obtain revised estimates of Ω_0 and X_2. To that end values of

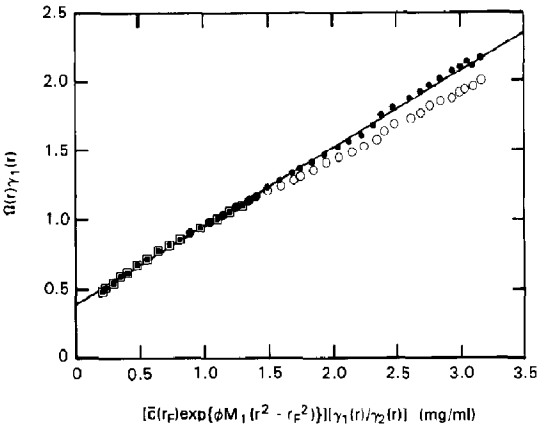

Fig. 2. Determination of a dimerization constant by application of eq. (10) with $\bar{c}(r_F) = 1.1$ mg/ml to Rayleigh interferograms of sedimentation equilibrium distributions for α-chymotrypsin in acetate–chloride, pH 3.9, I 0.2 [25]. Open symbols denote the initial analysis of two separate experiments on the basis of thermodynamic ideality, whereas solid symbols incorporate allowance for effects of non-ideality on the basis of the initial analysis and activity coefficients calculated via eqs. (13a–e).

2.44 and 3.07 nm have been ascribed to R_1 and R_2, respectively, on the basis of spherical geometry ($R_2 = 2^{1/3}R_1$) and substitution of the hydrodynamic radius for the effective thermodynamic radius of the hydrated monomer [29,30]. The respective nett charges of monomeric and dimeric α-chymotrypsin have been taken as +10 and +20 [31]. From the consequent reanalysis, signified by solid symbols in Fig. 2, Ω_0 decreases to 0.390 ± 0.023, whereas X_2 increases to 3.70 ± 0.80 L/g. On the grounds that iteration of the analysis leads to unchanged magnitudes for these two parameters, we conclude that $X_2 = 3.7 \pm 0.8$ L/g for the dimerization of α-chymotrypsin in acetate–chloride buffer, pH 3.9, I 0.20. Although smaller uncertainties were assigned to earlier estimates of X_2 for α-chymotrypsin under these conditions [25,29], the quoted precision took no account of uncertainty in Ω_0. The estimated error (± 2 S.E.M.) is therefore a more realistic estimate of the experimental uncertainty inherent in the dimerization constant.

Although the revised procedure has avoided the complete reliance of the original analysis upon a value of Ω_0 obtained by curvilinear ex-

trapolation of the $\Omega(r) - \bar{c}(r)$ dependence [14], any experimental error in the selected value of $\bar{c}(r_F)$ does, of course, introduce systematic error into the abscissa and ordinate parameters of the revised plot (Fig. 2). However, because the reference position is not restricted to a single solute concentration, repetition of the analysis with a range of such values should eliminate dependence of the evaluated association constant upon the particular reference position $[r_F, \bar{c}(r_F)]$ selected. In the present instance the dimerization constant obtained from Fig. 2 also described those evaluated on the basis of any reference concentration between 0.8 and 1.5 mg/mL, the range of overlap in the high-speed and low-speed sedimentation equilibrium experiments.

Of interest in the present context of allowance for effects of thermodynamic nonideality is the result obtained by resort to the Adams–Fujita [23] approximation (eq. 11) for evaluating the activity coefficients required for application of eq. (10). With those substitutions eq. (10) becomes

$$\Omega(r)\exp\left[BM_1\bar{c}(r)\right] = \Omega_0 + X_2\Omega_0^2\bar{c}(r_F) \times \exp\left[\phi M_1(r^2 - r^2F) - BM_1\bar{c}(r)\right] \quad (14)$$

On the basis that a plot of $\Omega(r)\exp[BM_1\bar{c}(r)]$ *versus* $\bar{c}(r_F)\exp[\phi M_1(r^2 - r_F^2) - BM_1\bar{c}(r)]$ should be linear for a monomer–dimer system, magnitudes were assigned to the curve-fitting parameter, B, and the most appropriate value was identified as that yielding the best linear correlation coefficient. Allowance for the effects of nonideality in this manner yielded $B = 0.0044$, $\Omega_0 = 0.415$ and $X_2 = 3.1 \pm 0.6$ L/g. This estimate of the dimerization constant is slightly larger than that of 2.6 ± 0.5 L/g obtained on the basis of thermodynamic ideality, but slightly smaller than the value of 3.7 ± 0.8 L/g obtained by allowing for effects of non-ideality on the statistical mechanical basis of excluded volume. Inasmuch as the discrepancy between values after allowance for thermodynamic non-ideality could be decreased by increasing the magnitude of the curve-fitting parameter, it is worth noting that identification of the most appropriate value of B for this system on the basis of best linear fit is not really satisfactory, being reliant upon differences in the seventh decimal place of a correlation coefficient in the vicinity of 0.9989. Such discrimination between values of the curve-fitting parameter would be hazardous even if the quantitative expressions were exact, and clearly questionable when the expression being used is known to contain an inappropriate allowance for the composition dependence of activity coefficients. Nevertheless, although adoption of the Adams–Fujita [23] approach may be inferior to the calculation of activity coefficients on the basis of excluded volume for simple (two-state) systems, it does at least alter the magnitude of the self-association constant in the correct direction. Because some allowance for effects of thermodynamic nonideality is probably better than none, it can be argued that there is some merit in applying the Adams–Fujita approximation to more complicated (multiple-state) self-associating systems for which lack of information precludes the assignment of shapes and valences to the various polymeric states of the solute.

3.3 Two-state self-association involving higher polymers

Having established and demonstrated a procedure for characterizing monomer–dimer equilibria (Fig. 2), we now wish to focus attention on two-state self-associating systems in which the polymeric species is larger than dimer. From the general counterpart of eq. (10), namely,

$$\Omega_0\gamma_1(r) = \Omega_0 + X_n\Omega_0^n\left\{\bar{c}(r_F)\exp\left[\phi M_1(r^2 - r_F^2)\right]\right\}^{n-1} \times \left\{\gamma_1(r)/\gamma_2(r)\right\} \quad (15)$$

it is evident that the plot (Fig. 2) of $\Omega_0(r)\gamma_1(r)$ *versus* $\bar{c}(r_F)\exp[\phi M_1(r^2 - r_F^2)]$ is only linear for reversible dimerization ($n = 2$). A curvilinear plot therefore implies either the existence of two-state self-association involving a polymeric state larger than dimer ($n > 2$), or the existence of multiple polymeric states in association equilibrium with

monomer. In this section the former situation is considered, the latter possibility being the subject of Sections 3.4 and 3.5.

Comparison of eqs. (6) and (15) shows that two-state self-association may be distinguished from multiple-state self-association on the grounds that a linear plot emanates from eq. (15) for a two-state system provided that the appropriate value of n is selected for the abscissa parameter, $\{\bar{c}(r_F)\exp[\phi M_1(r^2 - r_F^2)]\}^{n-1}\{\gamma_1(r)/\gamma_n(r)\}$. This possibility is explored by analysis of data that have been simulated for a monomer–tetramer system ($n = 4$) based loosely on haemoglobin.

Sedimentation equilibrium distributions were simulated initially for an ideal monomer–tetramer self-associating system at 20°C on the basis of the following parameters: $M_1 = 16000$, $(1 - \bar{v}\rho_s) = 0.260$, $X_4 = 0.118$ L^{3}g^{-3} (equivalent to the value used in [15], 6.85 and 7.10 cm as radial extremities (r_m, r_b) of the liquid column, and angular velocities of 40000 and 18000 rpm to generate high-speed [32] and low-speed [33] patterns. Simulations were commenced by assigning a total solute concentration, $\bar{c}(r_b)$, at the base of the liquid column, and by solving the quartic equation

$$X_4[c_1(r_b)]^4 + c_1(r_b) - \bar{c}(r_b) = 0 \qquad (16)$$

to obtain $c_1(r_b)$. The equilibrium distributions of monomer and tetramer throughout the column were then calculated from eq. (4) on the grounds that $z_i(r) = c_i(r)$ for an ideal system. Non-ideality was then introduced into the system by assigning values of 2.00 and 3.12 nm to the respective radii of monomer and tetramer, both of which were considered to bear nett zero charge ($Z_1 = Z_4 = 0$). Iterative application of the counterparts of eqs. (13a–e) for a monomer–tetramer system with the thermodynamic activities of monomer and tetramer [$z_1(r)$, $z_4(r)$] taken as the respective initial estimates of $c_1(r)$ and $c_4(r)$ then yielded the theoretical sedimentation equilibrium distributions, $\bar{c}(r)$ *versus* r. These were converted to refractometric units on the basis of a fringe displacement of 0.0295 cm and a value of 4.00 for the number of fringes generated by 1 mg/mL solute. In accordance with the protocol adopted

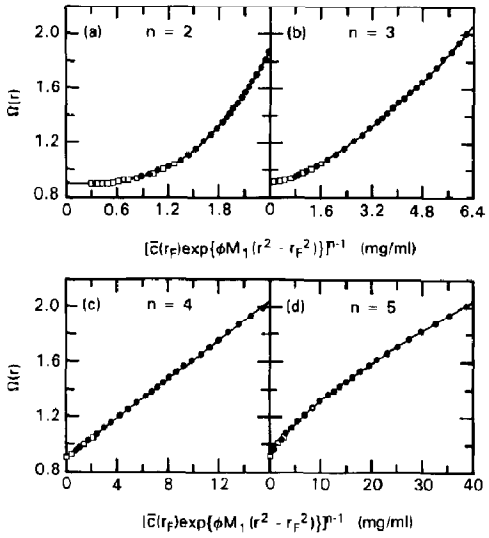

Fig. 3. Identification of the stoichiometry (n) of two-state self-association when the polymeric state of the solute is larger than dimer, simulated results for a thermodynamically non-ideal monomer–tetramer system being plotted in accordance with eq. (15) and a range of values (2–5) for n.

in [15], the uncertainty associated with experimental measurement of sedimentation equilibrium distributions was incorporated by superimposing on the distribution a random error with a standard deviation of 3 μm. The resulting distributions were then regarded as the simulated counterparts of experimental data for assessing the potential of the suggested analytical procedure for the recognition and characterization of the self-associating system giving rise to a particular set of sedimentation equilibrium distributions.

As predicted by eq. (15), the plot of $\Omega(r)$ *versus* $\bar{c}(r_F)\exp[\phi M_1(r^2 - r_F^2)]$ exhibits pronounced curvilinearity (Fig. 3a), whereupon it becomes of paramount importance to determine whether such plots based on thermodynamic ideality suffice to identify the appropriate value of n (*i.e.*, the stoichiometry of the two-state self-association) before the complicated allowance for effects of thermodynamic non-ideality needs to be introduced. The feasibility of identifying the magnitude of n by this means is illustrated in Fig. 3, where the relevant plots of the simulated data according to eq. (15) with $\gamma_1(r) = \gamma_n(r) = 1$ are presented for $n = 3$ (Fig. 3b), $n = 4$ (Fig. 3c) and

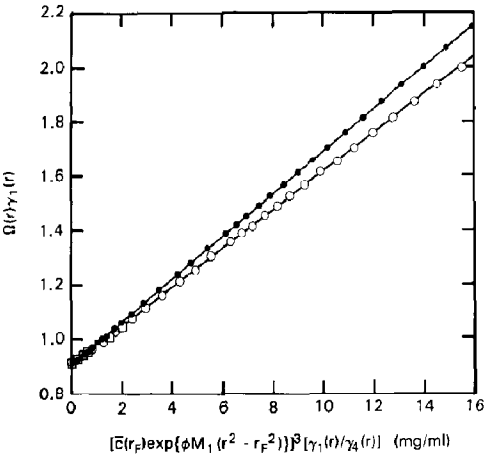

Fig. 4. Application of eq. 15 with n = 4 to data from simulated sedimentation equilibrium distributions to illustrate determination of the monomer–tetramer equilibrium constant for the system considered in Fig. 3. As in Fig. 2, open symbols denote the initial analysis of high-speed (squares) and low-speed (circles) experiments on the basis of thermodynamic ideality; and solid symbols the final analysis after correction for effects of thermodynamic nonideality via eqs. (13a–e).

$n = 5$ (Fig. 3d). Identification of the stoichiometry of two-state self-association as four is clearly established by these plots, despite their failure to take into account the effects of thermodynamic non-ideality. This finding simplifies greatly the allowance for effects of thermodynamic non-ideality, because the iterative approach adopted in relation to Fig. 2 for the α-chymotrypsin system needs to be applied for only a single value, *i.e.*, 4, of n. Whereas analysis of the results on the basis of ideality for a monomer–tetramer system (Fig. 4, open symbols) yielded $\Omega_0 = 0.901 \pm 0.010$ and $X_4 = 0.108 \pm 0.004$ L^3g^{-3}, allowance for effects of thermodynamic nonideality (via the counterparts of eqs. 13a–e) leads to the solid symbols in Fig. 4 and values of 0.902 ± 0.004 and 0.119 ± 0.007 L^3g^{-3} for Ω_0 and X_4 respectively. The latter is clearly an excellent estimate of the monomer–tetramer association constant (0.118 L^3g^{-3}) used to generate the simulated sedimentation equilibrium distributions.

3.4 Multiple-state self-association

Whenever polymeric species larger than dimer are formed there is a distinct possibility that the self-association is not simply a two-state equilibrium between monomer and a single higher polymeric species. In principle, the characterization of such systems with multiple polymeric states requires analysis in terms of eq. (6); but in practice it is probably more realistic to disregard the effects of thermodynamic non-ideality initially so that the number of parameters to be evaluated is decreased. Although there are many reported characterizations of non-ideal, multi-state self-associations, such analyses are based upon use of the Adams–Fujita approximation (eq. 11), for which there is no real justification in the case of globular proteins. Adoption of the concept of spherical geometry would certainly allow the predictions of all $\gamma_i(r)$ by means of an extended form of eq. (13) to include terms for all species in each activity coefficient; but this assumption becomes an increasingly uncertain approximation with increasing magnitude of i. At this stage we therefore opt for neglect of thermodynamic non-ideality, in which case eq. (6) becomes

$$\begin{aligned}\Omega_0(r) &= \Omega_0 + X_2\Omega_0^2\{\bar{c}(r_F)\exp(\phi M_1(r^2 - r_F^2))\} \\ &\quad + X_3\Omega_0^3\{\bar{c}(r_F)\exp(\phi M_1(r^2 - r_F^2))\}^2 \\ &\quad + X_4\Omega_0^4\{\bar{c}(r_F)\exp(\phi M_1(r^2 - r_F^2))\}^3 + \cdots \end{aligned} \quad (17)$$

The analysis of this situation is analogous to that for eq. (9) except that the dependence of $\Omega(r)$ on $\bar{c}(r_F)\exp[\phi M_1(r^2 - r_F^2)]$ is now described by a polynomial rather than a linear relationship. Adaptation of eq. (17) to describe systems devoid of specific polymeric species may be effected by setting $X_i = 0$ for the particular i-mer whose existence is to be neglected. Alternatively, the essential absence of a particular polymeric state may, in principle, be inferred from the return of a value of X_i that is indistinguishable from zero.

To illustrate the approach for characterizing multi-state self-association, sedimentation equilibrium distributions were simulated for a range of monomer–dimer–trimer systems. As before, the radial limits of the liquid column were set at 6.85 and 7.10 cm, and angular velocities of 40 000

and 18000 rpm were again used to generate the high-speed and low-speed sedimentation equilibrium distributions for these systems with a monomeric molecular weight of 16000. Monomer concentration at the cell base was taken as 1.0 mg/mL in simulations of high-speed experiments, and as 2.0 mg/mL in their low-speed counterparts. Results of the suggested analysis of these simulated distributions are summarized in Table 1 for a range of association constants (columns 1 and 2). The corresponding solute composition at the cell base (r_b) in each experiment is also included in Table 1 (next three columns) to allow ready appraisal of the maximal extent to which dimeric and trimeric species were present. Comparison of the evaluated associated constants (final two columns) with their corresponding input values is sufficiently favourable to justify optimism that relatively simple multi-state self-association equilibria can be identified and characterized by polynomial curve-fitting of the dependence of $\Omega(r)$ upon $\bar{c}(r_F)\exp[\phi M_1(r^2 - r_F^2)]$. In that regard it is pleasing to note that the polynomial approach to analyzing the data for the earlier monomer–tetramer system (Figs. 3 and 4 but with $\gamma_1(r) = \gamma_4(r) = 1$) also allowed its identification as a two-state self-association, because the values of X_2 and X_3 so deduced were effectively zero (but with uncertainties that were orders of magnitude greater than the evaluated parameters).

3.5 Indefinite self-association

An obvious problem in the characterization of self-association equilibria by non-linear regression analysis in terms of a general polynomial is the ever-increasing uncertainty associated with the magnitudes of successive equilibrium constants – a consequence of the incorporation of Ω_0 to the nth power in the polynomial coefficient ($X_n\Omega_0^n$). Consequently, with increasing n the stage is inevitably reached where the general polynomial approach fails to define the stoichiometric association constant (X_n) with an acceptable degree of precision. This situation, which pervades all analyses of multiple self-association equilibria, has prompted the introduction of models which place no restriction on the ultimate extent of self-association (upper limit of n); but which, of

Table 1

Evaluation of association constants for monomer–dimer–trimer systems by omega analysis of simulated sedimentation equilibrium distributions

Input constants		$c_i(r_b)$ (mg/ml) [a]			Evaluated constants [b,c]	
X_2 (L g^{-1})	X_3 (L^2 g^{-2})	$c_1(r_b)$	$c_2(r_b)$	$c_3(r_b)$	X_2 (L g^{-1})	X_3 (L^2 g^{-2})
0.12	0.30	1.00	0.12	0.30	0.116	0.297
		2.00	0.48	2.40		
0.02	0.40	1.00	0.02	0.40	0.016	0.396
		2.00	0.08	3.20		
0.40	0.20	1.00	0.40	0.20	0.394	0.198
		2.00	1.60	1.60		
0.50	0.06	1.00	0.50	0.06	0.494	0.0598
		2.00	2.00	0.48		
0.50	0.01	1.00	0.50	0.01	0.494	0.0104
		2.00	2.00	0.08		

[a] In each case the first entry refers to a simulated high-speed experiment (40000 rpm) with radial extremites (r_m, r_b) of 6.85 and 7.10 cm for the liquid column: the second entry refers to a corresponding simulation of a low-speed experiment (18000 rpm).

[b] Association constants determined by nonlinear curve-fitting of the dependence of $\Omega(r)$ upon $c(r_F)\exp[\phi M_1(r^2 - r_F^2)]$ in terms of a quadratic polynomial (eq. 17).

[c] Uncertainty in estimated values is less than 1 in the final decimal place.

necessity, impose restrictions on the relative magnitudes of the equilibrium constants describing successive self-association steps [7,34–37]: in isodesmic models all self-association steps are governed by the same molar equilibrium constants, whereas in attenuated models the equilibrium constants decrease systematically to allow for a varying entropy change at each step. For purposes of illustration we shall restrict consideration to application of the revised omega analysis for the characterization of the former systems.

For the simplest isodesmic model [34], involving indefinite self-association of monomer, the expression relating monomer concentration, $c_1(r)$, at radial distance r to the corresponding total concentration, $\bar{c}(r)$, is [34]

$$\bar{c}(r) = c_1(r)/\left[1 - k_i c_1(r)\right] \text{ for } k_i c_1(r) < 1 \tag{18}$$

where k_i is the molar isodesmic association constant divided by monomer molecular weight to allow expression of the relationship in terms of weight-concentrations: the absence of activity coefficients signifies assumed thermodynamic ideality. Combination of this expression with eq. (2a) (after noting the identity of $c_1(r)$ and $z_1(r)$ for an ideal system) and eq. (3) leads to the conclusion that

$$1/\Omega(r) = (1/\Omega_0) - k_i \bar{c}(r_F)\exp\left[\phi M_1\left(r^2 - r_F^2\right)\right] \tag{19}$$

Conformity with this simplest isodesmic model may thus be recognized by linear dependence of $1/\Omega(r)$ upon $\bar{c}(r_F)\exp[\phi M_1(r^2 - r_F^2)]$, in which case the isodesmic association constant (k_i) is obtained from the slope.

The application of this approach is illustrated in Fig. 5a, which summarizes reanalysis of Rayleigh interferograms, in accordance with eq. (19), of sedimentation equilibrium distributions for diisopropyl-α-chymotrypsin in dilute phosphate buffer, pH 7.9, I 0.03 [38]. Although this simplest example of isodesmic indefinite self-association has been invoked for α-chymotrypsin under similar conditions [39,40], the curvilinear form of Fig. 5a is clearly at variance with the linear dependence predicted by eq. (19) for such a system. Because α-chymotrypsin is known to form a symmetrical dimer [41], we explore models in which dimer (rather than monomer) undergoes isodesmic indefinite self-association.

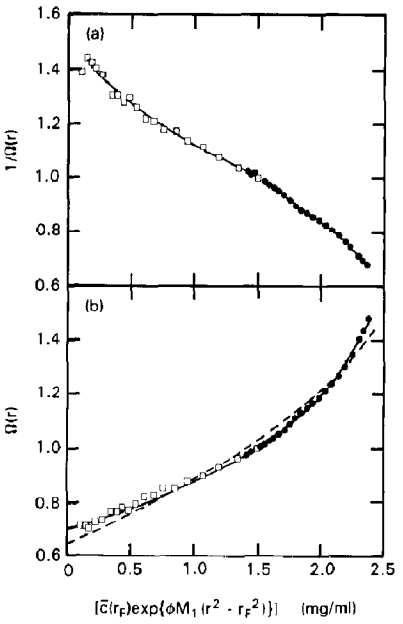

Fig. 5. Revised omega analysis, with $\bar{c}(r_F) = 1.5$ mg/mL, of sedimentation equilibrium distributions [38] for diisopropyl-α-chymotrypsin in dilute phosphate buffer (pH 7.9, I 0.03) in accordance with various models involving isodesmic self-association. (a) Test for conformity with the simplest model (eq. 19). (b) Non-linear regression analysis of results in terms of eqs. 20b (– – –) and 21b (—) for models involving isodesmic self-association of dimer.

Closed solutions for the description of total solute concentration in terms of that of monomer have been obtained for two types of isodesmic self-association that do not involve odd-numbered polymeric species. In the particular circumstance where the molar constant for dimerization also describes the isodesmic indefinite self-association of dimer, the analogs of eqs. (18) and (19) are [35,36]

$$\bar{c}(r) = c_1(r)\left[1 + \frac{2k_i c_1(r)}{\left(1 - k_i^2 c_1(r)^2\right)^2}\right] \quad \text{for} \quad k_i c_1(r) < 1 \tag{20a}$$

$$\Omega(r) = \Omega_0\left[1+\frac{2k_i\Omega_0\bar{c}(r_F)\exp[\phi M_1(r^2-r_F^2)]}{(1-k_i^2\Omega_0^2\{\bar{c}(r_F)\exp[\phi M_1(r^2-r_F^2)]\})^2}\right] \quad (20b)$$

Alternatively, if dimer formation entails discrete self-association that is governed, as before, by dimerization constant X_2, the corresponding expressions are [35,36,38]

$$\bar{c}(r) = c_1(r)\left[1+\frac{4X_2c_1(r)}{\left(2-X_2k_ic_1(r)^2\right)^2}\right] \quad (21a)$$

$$\Omega(r) = \Omega_0\left[1+\frac{4X_2\Omega_0\bar{c}(r_F)\exp[\phi M_1(r^2-r_F^2)]}{\left[2-X_2k_i\Omega_0^2\{\bar{c}(r_F)\exp[\phi M_1(r^2-r_F^2)]\}^2\right]^2}\right] \quad (21b)$$

Although the dependence of $\Omega(r)$ upon $\bar{c}(r_F)\exp[\phi M_1(r^2-r_F^2)]$ is predicted to be curvilinear for either model, it is evident from Fig. 5b that non-linear regression analysis in terms of eq. (21b) leads to much better description of the data (solid line) than the corresponding analysis in terms of eq. (20b) (dashed line). In that regard the consequent conclusion that the self-association of diisopropyl-α-chymotrypsin under these conditions is best described by a model involving discrete dimerization ($X_2 = 0.31 \pm 0.03$ L/g) followed by isodesmic indefinite association of dimer ($k_i = 0.70 \pm 0.09$ L/g) was also reached previously [38] by a much less sophisticated analysis that gave no indication of likely experimental uncertainty ($X_2 = 0.24$ L/g, $k_i = 0.68$ L/g).

4. Quantification by simulation

From the viewpoint of processing the experimental data to evaluate the self-association constant(s), the omega method clearly avoids the distortion of experimental uncertainty inherent in analysis based on differentiation of the logarithmic transform of the recorded sedimentation equilibrium distribution. However, as noted by Morris and Ralston [17,18], there remains the problem that uncertainty in the magnitude of $\bar{c}(r_F)$ is propagated as a systematic error. The approach adopted above for minimizing that factor in the treatment of α-chymotrypsin dimerization (Fig. 2) was to repeat the analysis with several $\bar{c}(r_F)$ values in the range of $\bar{c}(r)$ common to the high- and low-speed sedimentation equilibrium experiments. An alternative procedure is to identify the magnitude of the self-association constant by simulation techniques [11,15]. Of the two such approaches that have been recommended, one is based on simulation of the experimentally recorded sedimentation equilibrium distributions [15], whereas the other entails the matching of simulated and evaluated concentration dependences of weight-average molecular weight [11]. On the grounds that the goal of simulations should be the emulation of the experimentally observed phenomenon rather than a relationship derived therefrom by differentiation of a logarithmic transform of the experimental record, we conclude this study by illustrating an approach for identifying the dimerization constant for α-chymotrypsin dimerization (pH 3.9, I 0.2) by simulation of the $\bar{c}(r)$–r distributions. Although it lacks the sophistication and elegance of its predecessor [15], the present procedure does have the merit of avoiding the Adams–Fujita approximation [23] in the allowance for effects of thermodynamic non-ideality.

Simulations were commenced by selecting a reference concentration, $\bar{c}(r_F)$, that was common to the high- and low-speed sedimentation equilibrium distributions used for the omega analysis. Secondly, a magnitude was assigned to the thermodynamic dimerization constant, X_2, to allow first estimates of $c_1(r_F)$ and $c_2(r_F) = \bar{c}(r_F) - c_1(r_F)$ to be calculated by solving the quadratic

$$X_2^{app}[c_1(r_F)]^2 + c_1(r_F) - \bar{c}(r_F) = 0 \quad (22)$$

on the basis of thermodynamic ideality ($X_2^{app} = X_2$). These values of the two concentrations were used in conjunction with eqs. (13a–e) to give the estimates of $\gamma_i(r_F)$ ($i = 1,2$) required for evaluation of a second estimate of X_2^{app} via eq. (12). Its substitution into eq. (22) then led to revised estimates of the two species concentrations, the two

activity coefficients, and hence apparent dimerization constant associated with total concentration $\bar{c}(r_F)$. This step was repeated until further iteration produced no changes in the magnitudes of parameters.

Having established the concentrations and activity coefficients of monomer and dimer for a system with total concentration $\bar{c}(r_F)$ and the assigned association constant X_2, we were in a position to employ the basic sedimentation equilibrium expression to define theoretical distributions in terms of thermodynamic activities (eq. 23).

$$z_i(r) = z_i(r_F)\ \exp\{\phi M_i(r^2 - r_F^2)\}$$
$$\text{for } i = 1,2 \qquad (23)$$

In these calculations the values of radial distance coincided with those for which experimental measurements of $\bar{c}(r)$ were available. The two activities, $z_1(r)$ and $z_2(r)$, at each radial distance were then converted to the corresponding weight concentrations, $c_i(r) = z_i(r)/\gamma_i(r)$, by iterative application of eqs. (13a–e) with $z_1(r)$ and $z_2(r)$ as the initial estimates of the two concentrations. The concentrations $c_1(r)$ and $c_2(r)$ thus obtained were then summed at each radial distance to yield the array of theoretical total concentrations to be compared with their experimental counterparts. Finally, selection of the most appropriate assigned value of X_2 was assessed by subjecting the two sets of total concentration to linear regression analysis, and recognizing the association constant for α-chymotrypsin dimerization as the value of X_2 for which the slope equalled unity.

The dependence of the regression coefficient upon the value of X_2 selected for simulation is shown in Fig. 6 for $\bar{c}(r_F)$ values of 0.84 (dashed line), 1.10 (solid line), and 1.53 (dotted line mg/mL in the high- and low-speed sedimentation equilibrium experiments with an overlapping concentration range of 0.8–1.6 mg/mL. From the vertical lines, which signify the corresponding magnitudes of X_2 for a slope of unity, association constants of 2.9, 3.4 and 3.8 L/g are obtained for the dimerization of α-chymotrypsin by simulations based on these three $\bar{c}(r_F)$ values. Inasmuch as a dimerization constant of 3.7 ($\pm$0.8) L/g was

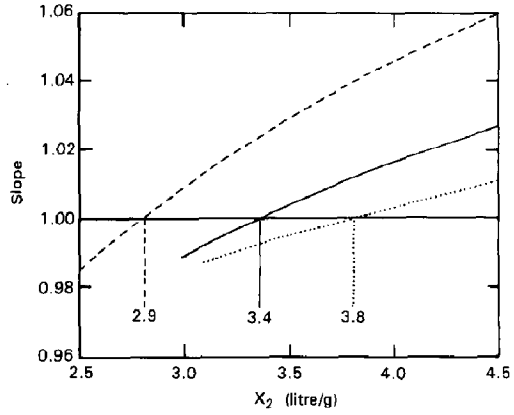

Fig. 6. Dependence of the slope of the linear relationship between theoretical and experimental values of the total concentration, $\bar{c}(r)$, upon the magnitude of the dimerization constant, X_2, assigned for simulation of the sedimentation equilibrium distributions obtained with α-chymotrypsin in acetate-chloride buffer, pH 3.9, I 0.2. Numbers indicate the magnitudes of the dimerization constant (L/g) obtained as the value of X_2 for which the slope is unity from simulations based on reference concentrations, $c(r_F)$ of 0.84 (– – –), 1.10 (—) and 1.53 (· · ·) mg/ml.

obtained by omega analysis (Fig. 2), it is evident that comparable quantification is obtained by either approach. Such a conclusion is not surprising in view of the fact that both procedures are based on direct application of the sedimentation equilibrium expression in its untransformed state.

5. Concluding remarks

This investigation has served to re-emphasize the potential of the omega function [14] for characterizing solute self-association, and to present an improved form of its application. The activity coefficient of a non-associating solute may be determined from the linear dependence of $\Omega(r)$ upon $\bar{c}(r)$ (eq. 8 and Fig. 1); and, in principle, the equilibrium constant for ideal dimerization, may be quantified by linear regression analysis of the dependence of $\Omega(r)$ upon $\bar{c}(r_F)\exp[\phi M_1(r^2 - r_F^2)]$ (eq. 9). Thermodynamic non-ideality introduces curvilinearity (possibly undetectable) into the plot for a monomer–dimer system; but the value of the apparent association constant deduced therefrom allows calculation of activity co-

efficients on the statistical-mechanical basis of excluded volume [21], and hence reappraisal of the data with allowance made for the effects of thermodynamic non-ideality (Fig. 2). In the event that the polymeric state is larger than dimer, the plot of $\Omega(r)$ *versus* $\bar{c}(r_F)\exp[\phi M_1(r^2 - r_F^2)]$ exhibits upward curvilinearity (Fig. 3a) because $\Omega(r)$ varies linearly with the $(n-1)$th power of the abscissa parameter (eq. 15). A series of plots with a range of potential n values should allow identification of the stoichiometry (Fig. 3) and hence of X_n (Fig. 4).

Systems exhibiting self-association equilibria involving multiple polymeric states may be recognized by the inability to find any value of n that leads to linearization of the dependence of $\Omega(r)$ upon $\{\bar{c}(r_F)\exp[\phi M_1(r^2 - r_F^2)]\}^{n-1}$. If the self-association pattern involves relatively few polymeric solute states the system may be characterized by general polynomial curve-fitting of the curvilinear dependence of $\Omega(r)$ upon $\bar{c}(r_F)\exp[\phi M_1(r^2 - r_F^2)]$ (Table 1). The requirement to extend such an analysis beyond a few values of n places the researcher in a dilemma, because adoption of a general model involving a large number of polymeric species automatically leads to ambiguous description of the self-association through inability to define adequately the successive equilibrium constants. A corollary of that inference is that retention of all polymeric species can only be encompassed by imposing restrictions on the relative magnitudes of successive self-association constants. Consequently, even though the various models based on indefinite self-association [7,34–37] are open to criticism on the grounds that the major justification for their application is simply the availability of a quantitative description of solute concentration in closed form, resort to some such simplification of the relationship(s) between the relative magnitudes of successive equilibrium constants is likely to be mandatory for a reasonably definitive quantitative description to be obtained of solute self-association involving a large number of polymeric states. The omega analysis also finds ready application to these systems, as is evident from the consideration of results for diisopropyl-α-chymotrypsin at low ionic strength in terms of isodesmic models (Fig. 5). Finally, the equivalence of quantitative inferences stemming from the omega analysis and the simulation of concentration distributions at sedimentation equilibrium [15] has been illustrated by an adaptation of the latter procedure to obtain the dimerization constant for α-chymotrypsin in acetate–chloride buffer, pH 3.9, I 0.2 (Fig. 6). The only difference between the two approaches is that the omega analysis employs the experimental data for evaluation of the equilibrium constant, whereas the simulation procedure identifies it by screening an array of potential association constants for conformity with the experimental sedimentation equilibrium distribution(s).

Acknowledgements

We wish to thank Drs. G.B. Ralston and M. Morris for helpful discussions of this manuscript. The support of this investigation by a grant from the Australian Research Council is also gratefully acknowledged.

References

1 E.T. Adams Jr. and J.W. Williams, J. Am. Chem. Soc. 86 (1964) 3454.
2 P.D. Jeffrey and J.H. Coates, Biochemistry 5 (1966) 489.
3 D.E. Roark and D.A. Yphantis, Ann. N.Y. Acad. Sci. 164 (1969) 245.
4 V.D. Hoagland and D.C. Teller, Biochemistry 8 (1969) 594.
5 K.E. Van Holde, G.P. Rosetti and R.D. Dyson, Ann. N.Y. Acad. Sci. 164 (1969) 279.
6 M.S. Lewis and G.D. Knott, Biophys. Chem. 5 (1976) 171.
7 L.-H. Tang, D.R. Powell, B.M. Escott and E.T. Adams, Jr., Biophys. Chem. 7 (1977) 121.
8 H. Kim, R.C. Deonier and J.W. Williams, Chem. Rev. 11 (1977) 659.
9 W.F. Stafford, III, Biophys. J. 29 (1980) 149.
10 E. Bucci, Biophys. Chem. 24 (1986) 47.
11 R.C. Chatelier and A.P. Minton, Biopolymers 26 (1987) 507.
12 R.F. Steiner, Arch. Biochem. Biophys. 39 (1952) 333.
13 D.C. Teller, Methods Enzymol. 27 (1973) 346.
14 B.K. Milthorpe, P.D. Jeffrey and L.W. Nichol, Biophys. Chem. 3 (1975) 169.
15 M.L. Johnson, J.J. Correia, D.A. Yphantis and H.R. Halvorson, Biophys. J. 36 (1981) 575.

16 A.P. Minton, Anal. Biochem. 190 (1990) 1.
17 M. Morris and G.B. Ralston, Biophys. Chem. 23 (1985) 49.
18 M. Morris and G.B. Ralston, Biochemistry 28 (1989) 8561.
19 M. Fixman, J. Phys. Chem. 62 (1958) 374.
20 H. Eisenberg, Biological macromolecules and polyelectrolytes in solution (Clarendon Press, Oxford, 1976).
21 P.R. Wills and D.J. Winzor, in: Ultracentrifugation in biochemistry and polymer science, eds. S.E. Harding and A.J. Rowe (Roy. Soc. Chem., London), in press.
22 P.D. Jeffrey, L.W. Nichol, D.R. Turner and D.J. Winzor, J. Phys. Chem. 81 (1977) 776.
23 E.T. Adams Jr. and H. Fujita, in: Ultracentrifugal analysis in theory and experiment, ed. J.W. Williams (Academic Press, New York, 1963) p. 119.
24 A.G. Ogston and D.J. Winzor, J. Phys. Chem. 79 (1975) 2496.
25 R. Tellam, J. de Jersey and D.J. Winzor, Biochemistry 18 (1979) 5316.
26 D.J. Winzor and H.A. Scheraga, J. Phys. Chem. 68 (1964) 338.
27 K.C. Aune and S.N. Timasheff, Biochemistry 10 (1971) 1609.
28 T.A. Horbett and D.C. Teller, Biochemistry 13 (1974) 5490.
29 K.E. Shearwin and D.J. Winzor, Biophys. Chem. 31 (1988) 287.
30 K.E. Shearwin and D.J. Winzor, Eur. J. Biochem. 190 (1990) 523.
31 C.L. Ford and D.J. Winzor, Biochim. Biophys. Acta 756 (1983) 49.
32 D.A. Yphantis, Biochemistry 3 (1964) 297.
33 K.E. Van Holde and R.L. Baldwin, J. Phys. Chem. 62 (1958) 734.
34 K.E. Van Holde and G.P. Rossetti, Biochemistry 6 (1967) 2189.
35 E.T. Adams Jr., W.E. Ferguson, P.E. Wan, J.L. Sarquis and B.M. Escott, Sep. Sci. 10 (1975) 175.
36 F. Garland and S.D. Christian, J. Phys. Chem. 79 (1975) 1247.
37 J.M. Beckerdite, C.C. Wan and E.T. Adams Jr., Biophys. Chem. 12 (1980) 199.
38 R. Tellam and D.J. Winzor, Biochem. J. 161 (1977) 687.
39 M.W. Pandit and M.S.N. Rao, Biochemistry 13 (1974) 1048.
40 M.W. Pandit and M.S.N. Rao, Biochemistry 14 (1975) 4106.
41 T.A. Steitz, R. Henderson and D.M. Blow, J. Mol. Biol. 46 (1969) 337.